Determination of the g Tensors for the Dominant Stable Radicals in X-Irradiated β-D-Fructose Single Crystals

Mihaela Adeluta Tarpan,[†] Henk Vrielinck,[‡] Hendrik De Cooman,[†] and Freddy Callens*

Department of Solid State Sciences, Ghent University, Krijgslaan 281-S1, B-9000 Gent, Belgium

Received: February 24, 2009; Revised Manuscript Received: May 28, 2009

In spite of recent successful identifications of radicals produced after X-ray irradiation at 10 and 77 K in β-D-fructose, the structure of the two stable radicals dominating the electron paramagnetic resonance (EPR) spectrum after room temperature irradiation is still unclear. Based on the agreement between proton hyperfine (HF) tensors obtained in electron nuclear double resonance (ENDOR) experiments and the results of single molecule density functional calculations, a model for these radicals, involving OH abstraction at the C2 ring position, had previously been proposed, but this assignment could not be confirmed when the radical was embedded in a crystal environment. In this paper, we therefore provide additional experimental information for these radicals. First, their **g** tensors are determined from angular dependent ENDOR-induced EPR experiments. The relatively large anisotropy of these tensors is indicative of delocalization of the unpaired electron onto a neighboring oxygen atom. Second, EPR spectra of fructose powders, selectively enriched in ^{13}C on various ring positions, are presented, demonstrating that the HF interaction with the carbon atom C3 is larger than with the C2. Combining the **g** tensor, proton and ^{13}C HF data, we conclude that the structure of the stable radicals differs strongly from that of intact molecules and that further advanced quantum chemical modeling will be required to fully identify them.

Introduction

Both as model systems for studying the effects of radiation on the DNA sugar unit and for applications in dosimetry, irradiated mono- and disaccharides, such as glucose,[1,2] fructose,[3−5] sucrose[6,7] and rhamnose,[8−13] have been intensively studied with electron paramagnetic resonance (EPR) over the past few decades. By now it is well-established that such EPR spectra are multicomposite. At room temperature (RT) the primary radiation products, which may be stabilized at low temperature, transform into stable radicals via multistep radical reaction mechanisms. The molecular structure and geometry of the latter may differ considerably from those of the intact molecules, even in the solid state (crystals). This was recently convincingly established for sucrose single crystals, where all three dominant stable radicals were shown to involve glycosidic bond rupture and carbonyl formation on a carbon atom adjacent to the main site of unpaired electron density.[7,14,15] A prominent radical in glucose-1-phosphate, detected at 77 K after *in situ* X-irradiation at 77 K, was also found to display these characteristics.[16,17] The structural identification of these radicals is in most cases the result of a combination of EPR and electron nuclear double resonance (ENDOR) experiments and theoretical calculations based on density functional theory (DFT), proton hyperfine (HF) interactions being the main source of information. Basically, a radical model is accepted when the DFT calculations on that model accurately reproduce the experimental proton HF tensors in both principal values and directions.

In spite of its relatively simple molecular and crystal structure (see Figure 1) and hence maybe contrary to expectations, β-D-fructose turns out to be a more difficult system with respect to identification of radiation-induced radicals. We recently successfully identified the dominant radical species after irradiation at 10 K in these crystals as resulting from net H-abstraction at two C atoms in the fructopyranose six-ring (C3 and C5).[5] An earlier study after irradiation at 77 K had demonstrated the presence of similar C3 centered, H-abstracted radicals, in addition to ring-opened species.[4] For the dominant RT stable radicals doubts have arisen concerning the model assignment, based on single molecule DFT calculations, involving an OH-abstraction at the C2 position.[2,3] Refinements of the calculations, embedding the radical in a cluster of neighbors or in a periodic lattice environment, were unable to reproduce the earlier reported excellent agreement with experiment, especially with respect to the HF tensor principal axes. Moreover, measurements on selectively ^{13}C enriched fructose powders, presented in this paper (see Experimental Results section), suggest that the radical might be centered at C3, rather than at C2. For these centers, the proton HF tensors apparently provide insufficient information to allow for identification.

In this paper, we analyze the **g** tensors for the F1 and F2 dominant stable radicals in β-D-fructose. These experimental parameters are not so often used in the identification of carbon centered radicals, because deviations from the free electron ***g*** value are usually quite small. Hence they are difficult to establish at standard microwave frequencies (X-band, 9.5 GHz) where the anisotropy is dominated by proton HF interactions. The already mentioned composite nature of the spectra, further complicated by the presence of site splitting when studying single crystals, renders an accurate determination of the radical **g** tensors even more difficult. These problems will only in part be solved by performing experiments at high microwave frequencies/high fields, which also bring about difficulties in sample preparation and orienting. Therefore, we have chosen here to determine **g** tensors by recording the angular dependence of ENDOR-induced EPR spectra (EIE). To our knowledge, the

* To whom correspondence should be addressed. Tel: +32 9 264 43 52. Fax: +32 9 264 49 96. E-mail: Freddy.Callens@ugent.be.
† Research assistant of the Flemish Research Foundation (FWO).
‡ Postdoctoral Fellow of the Flemish Research Foundation (FWO).

10.1021/jp9017019 CCC: $40.75 © 2009 American Chemical Society
Published on Web 06/26/2009

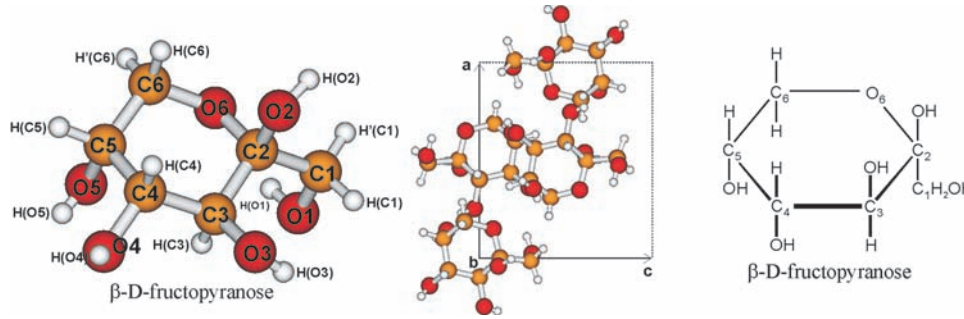

Figure 1. Left: Molecular structure of β-D-fructose with labeled atoms. Central: Four β-D-fructose molecules in the unit cell. Right: Fructose chemical structure.

only previous report of applying this method to radicals in organic crystals is by Kang et al.[18] They established that the method is reliable—EPR and EIE lead to identical **g** tensors—and effectively separates overlapping spectra. In order to enhance **g** tensor resolution, we performed the experiments at the microwave Q-band (34 GHz). Knowledge of the radical **g** tensors is also necessary if one aims at reproducing powder spectra,[19,20] e.g. in order to determine the contributions of various radicals for dose assessment. Finally, the Q-band powder EPR spectra of samples selectively ^{13}C enriched on different carbon positions are compared with that of the nonenriched sample.

Materials and Methods

The β-D-fructose powders (98% ^{12}C) and the fructose powder enriched with ^{13}C at C1 and C2 positions (99%) were purchased from Sigma-Aldrich and fructose powder enriched at C3, C4, C5 and C6 positions (99%) from Omicron Biochemicals. Single crystals of β-D-fructose were grown from saturated aqueous solutions containing ethanol by slow evaporation at 40 °C. β-D-Fructose crystals are orthorhombic with space group symmetry $P2_12_12_1$ and four molecules in the unit cell (Figure 1).[21,22] The crystal axes were labeled according to a neutron diffraction study,[22] i.e. $a = 0.9191$ nm, $b = 1.0046$ nm and $c = 0.8095$ nm. a, b and c were chosen as the reference axes for analyzing the EPR, ENDOR and EIE spectra.

For the identification of the crystal axes an X-ray diffractometer BRUKER D8 Discover was used. Based on the pole figures, the rotation axis for the EPR/ENDOR experiments was aligned within 1° along the a or b crystal axis. The third plane was slightly skewed and defined by the polar angles: $\theta = -9°$; $\phi = 1°$ (θ is the deviation angle of the rotation axis from the z axes, and ϕ is the angle measured from the x axis to the projection of the rotation axis in the xy plane). The crystals were then transferred and glued to quartz crystal holders without loss of alignment.

The samples were X-irradiated at RT with a dose of approximately 30 kGy using a Philips tungsten anticathode X-ray tube operated at 60 kV and 40 mA.

The Q-band EPR spectra were recorded using a Bruker Elexsys E500 Q-band spectrometer equipped with an Oxford CF935 cryostat. The magnetic field and the microwave frequency were measured using a Bruker ER035 M NMR gaussmeter and an EIP 548B microwave frequency counter, respectively. For absolute calibration of the field, a DPPH standard sample ($g = 2.0036$) was measured.

The EPR, ENDOR and EIE measurements were performed in the three mentioned planes by rotating the sample in 5° steps over 100° for the tilted ab and perfect bc plane and over 180° in the perfect ac plane. For simulations and fittings of EPR and EIE spectra and their angular variations, the EasySpin[23] routines in Matlab were used.

Extraction of the principal values and directions of a **g** tensor from the angular dependence of the EPR spectrum, or of a HF **A** tensor from ENDOR, in three planes may in general be subject to Schonland ambiguity.[24,25] For the proton HF tensors, we solved this problem by recording angular dependences in several additional tilted planes. Knowing the site assignation for the ENDOR transitions immediately lifts the degeneracy in EIE.

Experimental Results

All EPR, ENDOR and EIE measurements presented in this study were carried out at 55 K. A typical EPR spectrum consists of a considerable number of strongly overlapping broad resonances close to the free electron **g** value, as illustrated in Figure 2a. The EPR angular variation did not allow an accurate interpretation of the spectrum. Hence ENDOR and EIE measurements were started in order to enhance spectral resolution and to separate contributions originating from different radical species. From the angular variation of the well-resolved ENDOR lines, ten proton HF tensors were determined. In the present study we will concentrate on the five tensors corresponding to the proton HF interactions assigned to the radicals F1 and F2. Their principal values and directions are listed in Table 1 and are in excellent agreement with those reported in the work of Vanhaelewyn et al.[3] The other five newly determined HF tensors belong to four additional radical species and will be discussed in a future publication.

Both the F1 and F2 radicals exhibit two β-like proton HF couplings, a large coupling with an isotropic HF value around 100 MHz and a coupling of intermediate strength around 40 MHz, and a third, probably γ-type, small coupling around 10 MHz. For the radical F2 only the strong (HF1(F2)) and intermediate (HF2(F2)) HF tensors could be completely determined from the ENDOR angular variations. The smallest coupling could not be followed in enough planes to allow a complete determination of the hyperfine tensor. The close similarity of both principal values and direction cosines of the experimental hyperfine coupling tensors suggests that they belong to the same type of radical stabilized in two slightly different geometrical conformations.

The procedure followed to determine the **g** tensor from the angular dependence of the EIE spectrum is illustrated in Figures 2 and 3. The ENDOR spectrum in Figure 2b, recorded with the magnetic field aligned to the c axis at the EPR transition indicated in Figure 2a with an arrow, reveals transitions of both F1 and F2. Due to the similarity of the radicals, this is in general the case. The EIE spectra, like in Figure 2c, are recorded at the high frequency ENDOR lines of the two radicals (90−105

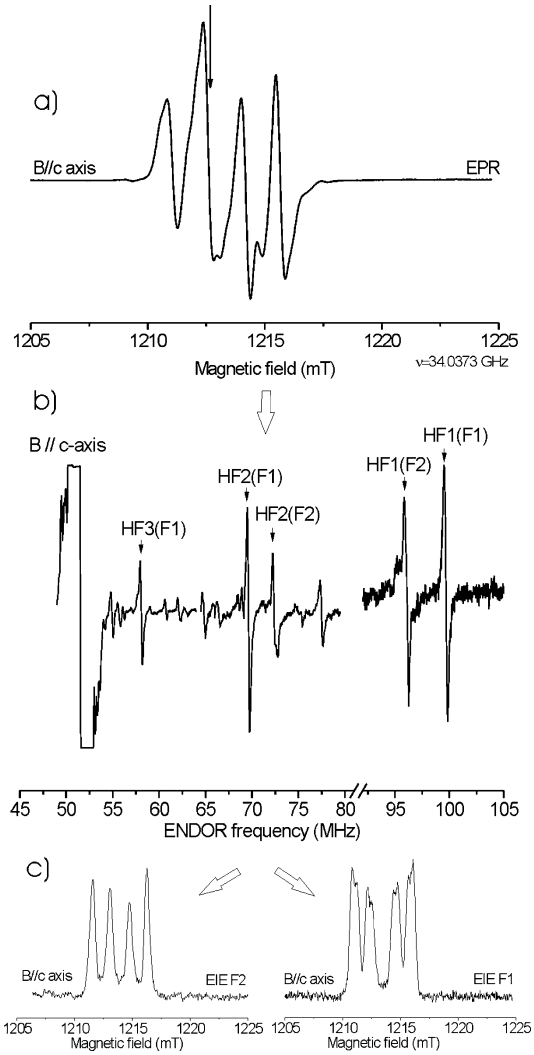

Figure 2. Q-band EPR (a), ENDOR (b) and EIE (c) spectra recorded at 55 K of RT X-irradiated β-D-fructose single crystals for the magnetic field parallel to the *c* axis. The ENDOR spectra were obtained with the magnetic field position locked to the EPR line marked by an arrow. The EIE spectra were obtained by monitoring the intensity of the ENDOR lines corresponding to the HF1(F1) and HF1(F2) proton HF interactions.

MHz). For a magnetic field orientation along one of the principal crystallographic axes, the EPR spectra of the four symmetry-related sites for a certain radical coincide. For orientations in the crystallographic *ab*, *bc* and *ca* planes, splitting in two symmetry related spectra occurs, and outside of these planes a splitting in four components even occurs. Therefore, ENDOR spectra have to be recorded at several magnetic field positions in the EPR spectrum. As an example, in Figure 3 the EIE spectra of the F1 radical recorded at the two symmetry related branches in the ENDOR spectrum in the *bc* plane (see Figure 4a, middle panel) are presented. The HF interactions are sufficiently small with respect to the microwave frequency to allow neglect of second order effects in EPR. Hence, the effective *g* factor for a certain site of a certain radical in a particular magnetic field orientation can be calculated from the center of the HF pattern in the EIE spectrum: $g = h\nu_{MW}/\mu_B B_0$. These B_0 positions are marked in Figure 3 with crosses and are represented by dots in Figures 4b and 4c.

For the *ac* and *bc* planes the EIE angular variation was performed for two distinct sites of the crystal, that are related by the orthorhombic symmetry transformation: $(x,y,z) \rightarrow (-x,-y,z)$. Because the third rotation axis is tilted away from the *c* axis ($\theta = -9°$ and $\phi = 1°$, see above), site splitting into four lines occurs. We restricted the EIE angular variation to two sites which are related by the orthorhombic symmetry operation: $(x,y,z) \rightarrow (x,-y,-z)$. By least-squares error fitting, we determined the **g** tensors of F1 and F2, as presented in Table 1. The simulated angular dependences of the central EIE resonance positions for the two radicals are represented by full lines in Figure 4 and match the experimental results excellently.

TABLE 1: Experimental Proton HF Tensors (MHz) and g Tensors for the F1 and F2 Radicals in RT X-Irradiated Fructose Single Crystals, Obtained from Q-Band ENDOR and EIE Measurements at 55 K[a]

			principal directions		
radical	tensor	principal values	*a*	*b*	*c*
F1	**g**(F1)	2.0019(1)	0.304(12)	0.939(7)	0.163(4)
		2.0054(1)	0.941(6)	−0.270(11)	−0.201(2)
		2.0042(2)	−0.145(10)	0.215(13)	−0.966(3)
	HF1(F1)	103.54(2)	0.504(1)	0.647(9)	0.572(3)
		93.64(2)	0.179(1)	−0.726(1)	0.664(8)
		92.19(2)	0.845(1)	−0.232(6)	−0.482(6)
	HF2(F1)	43.99(2)	0.887(1)	−0.097(4)	0.452(5)
		34.41(3)	0.363(2)	−0.460(14)	−0.811(7)
		33.22(3)	0.287(1)	0.883(6)	−0.372(13)
	HF3(F1)	14.03(3)	−0.140(5)	0.315(2)	−0.939(4)
		8.02(2)	0.912(2)	0.409(5)	0.002(3)
		5.51(2)	0.385(1)	−0.856(4)	−0.344(2)
F2	**g**(F2)	2.0019(2)	0.316(10)	0.833(12)	0.455(13)
		2.0052(1)	0.944(9)	−0.227(8)	−0.242(7)
		2.0040(1)	−0.098(11)	0.506(2)	−0.857(8)
	HF1(F2)	94.33(3)	0.612(1)	0.517(12)	0.599(2)
		84.23(3)	−0.066(2)	−0.721(14)	0.690(3)
		83.52(3)	0.788(1)	−0.461(13)	−0.407(2)
	HF2(F2)	49.55(3)	0.915(1)	0.038(2)	0.401(7)
		40.49(3)	0.385(3)	−0.375(15)	−0.843(6)
		39.12(3)	0.119(1)	0.926(6)	−0.358(14)

[a] The numbers in parentheses represent the uncertainty in the last significant digit(s). Principal directions are reported only for one of the symmetry related sites; the other sites can be obtained by performing the allowed symmetry operations: the 2-fold rotation around the *a* axis (the signs of *b* and *c* principal components are changed), around *b* (change the signs of the *a* and *c* components) and around *c* (change the signs of the *a* and *b* principal components).

In order to test the quality of the **g** and hyperfine data obtained for F1 and F2, a series of EIE and EPR spectrum simulations were performed. In Figure 5 the EIE spectra for magnetic field orientations along the three crystallographic axes for the F1 and F2 radicals are shown. Each experimental spectrum is accompanied by its simulation, and excellent agreement is found. Next, the total EPR spectra in the *a* and *c* directions are compared with simulations in Figure 6, assuming equal contributions from the two radicals. The spectrum in the *b* direction is excluded from the comparison, as in this orientation the third HF interaction for F2 gives rise to a resolved splitting (see Figure 5), but no HF tensor is available for simulating this splitting. For both orientations the agreement between the simulated and the experimental spectrum is fairly good, clearly indicating that F1 and F2 are indeed the dominant contributions to the spectrum. It is, however, also obvious that additional components are present, supporting our earlier conclusion from ENDOR that at least four other radical species are produced in fructose by RT irradiation.

Additional but still largely unexplored sources of information about the radical structure are the ^{13}C HF interactions. We performed EPR measurements on selectively ^{13}C enriched fructose powders at different ring positions with the primary aim of determining at which carbon atom the unpaired electron

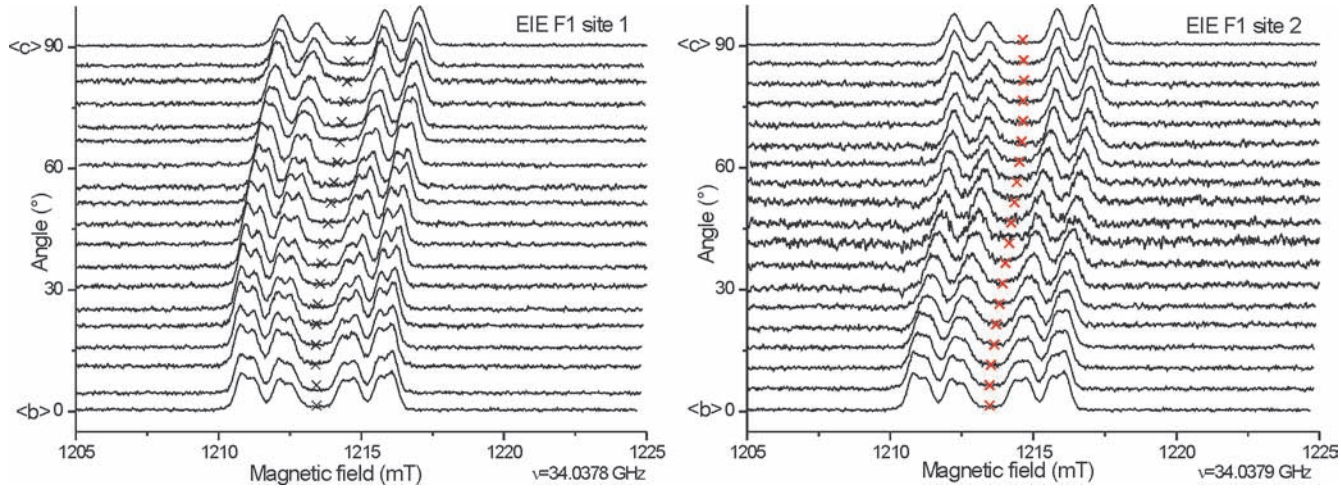

Figure 3. EIE angular dependence of the radical F1 measured by rotation about the *a* axis. The EIE angular variation was performed for two magnetically distinct sites, related by the orthorhombic symmetry transformation: $(x,y,z) \rightarrow (-x,-y,z)$. The $B_0 = h\nu_{MW}/\mu_B g_{eff}$ values are marked by black and red crosses for site 1 and site 2 respectively.

density is mainly localized. As the EPR spectrum of β-D-fructose single crystals is dominated by (approximately) equal contributions of the F1 and F2 radicals, one might expect the powder spectra will also be. Therefore, if fairly large changes in the EPR spectra of selectively enriched fructose powders occur, we may expect them to come from these two radicals and not from minority contributions. In Figure 7a the EPR spectra of nonenriched fructose powder and of six powders each enriched in a different carbon position are compared. For three selectively enriched samples the EPR spectra show no (enrichment at C5 and C6) or almost no changes (enriched at C1) when compared with the nonenriched sample. On the other hand the EPR spectra for the samples enriched at C2, C3 and C4 show significant changes with respect to their resolved structure, i.e. the contributions of F1 and F2. The experimental spectra recorded for the powders enriched at C2 and C4 resemble each other very well. However, the largest ^{13}C splitting for F1 and F2 is observed in the sample selectively enriched at C3: this EPR spectrum is approximately 2 mT wider than that for the powders enriched in C2 and C4. In Figure 7b a tentative simulation of the EPR spectrum of 3-^{13}C fructose powder is presented, using an axial hyperfine coupling tensor for ^{13}C, with the A_z (parallel) direction parallel to that of the minimum g value ($g_{min} = 2.0019$). The preliminary estimates for the ^{13}C HF values are $A_x = A_y \ll A_z = 160$ MHz (for the simulation presented in Figure 7b $A_x = A_y = 10$ MHz). The comparison with the experimental spectrum (repeated in Figure 7b) shows that a simulation with these HF values produces resolved structure in the right position, but the agreement for the relative line intensities and overall spectral shape is still rather poor. It should of course be considered that the restrictions we imposed on the HF tensor are rather severe and that, at this moment, the anisotropy of (the various sources of) line width broadening have not fully been explored. Moreover, the highly anisotropic ^{13}C HF coupling of the radicals F1 and F2 might favor the detection of minority species in the C3 enriched powder. Obtaining more reliable ^{13}C HF data for F1 and F2 will also imply additional experiments at other (higher) microwave frequencies.

Discussions

Obviously, the main goal of studying radicals in sugar crystals with EPR and ENDOR is to obtain structural models for the radiation-induced radicals. Our previous experimental and computational work on the RT stable radicals in fructose has, however, demonstrated that finding a suitable model is not at all trivial. In the following, we will first try to construct a radical fragment that would display the newly acquired and already established experimental characteristics of F1 and F2, based on literature data and semiempirical theory of carbohydrates radicals. Next, we will try and fit such a fragment in the fructose molecular crystal structure. The main conclusions of this procedure, however, turn out to be that the structure of F1 and F2 strongly deviate from that of the intact molecules. As a result, the approximations used might no longer be valid/useful for identifying these radicals.

Considering first the **g** tensor of F1 and F2 (Table 1), we note that its anisotropy is small, indicating that F1/F2 are indeed carbon-centered radical species. However, comparing the principal values of the **g** tensors of F1 and F2 with those of regular alkyl radicals (including R1−$\dot{C}$OH−R2 fragments, one may observe that the anisotropy is considerably larger. Such enhanced g anisotropy has been attributed to spin delocalization onto a neighboring oxygen atom, as e.g. discussed by Sagstuen et al. for one of the major radicals obtained after X-irradiation in sucrose single crystals.[26] The DFT identification by De Cooman et al. indeed proved that a carbonyl group is next to the central carbon atom in the T2/T3 radical.[14] The g anisotropy in this case was larger than what we observe for F1 and F2. Indeed, the experimental maximum g values (g_{max}) in Table 1 are slightly smaller than expected for such a fragment, which may point to a smaller spin density than usually found on the carbonyl group (∼0.30).[14,15] Hence, we arrive at a radical fragment structure of the form R1−(C═O)−$\dot{C}$R2R3.

Both F1 and F2 exhibit three proton hyperfine couplings. Judging by the principal values, the two larger couplings are of the beta type. The third, small coupling is most probably due to a gamma proton and shows isotropic and anisotropic values similar to those of the gamma couplings for the stable radicals in sucrose.[14,15]

The isotropic hyperfine coupling a^{β}_{iso} of a beta proton in a carbon-centered radical is given by the Heller−McConnell relation[27,28]

$$a^{\beta}_{iso} = \rho^{\pi}(B_0 + B_2 \cos^2 \theta) \quad (1)$$

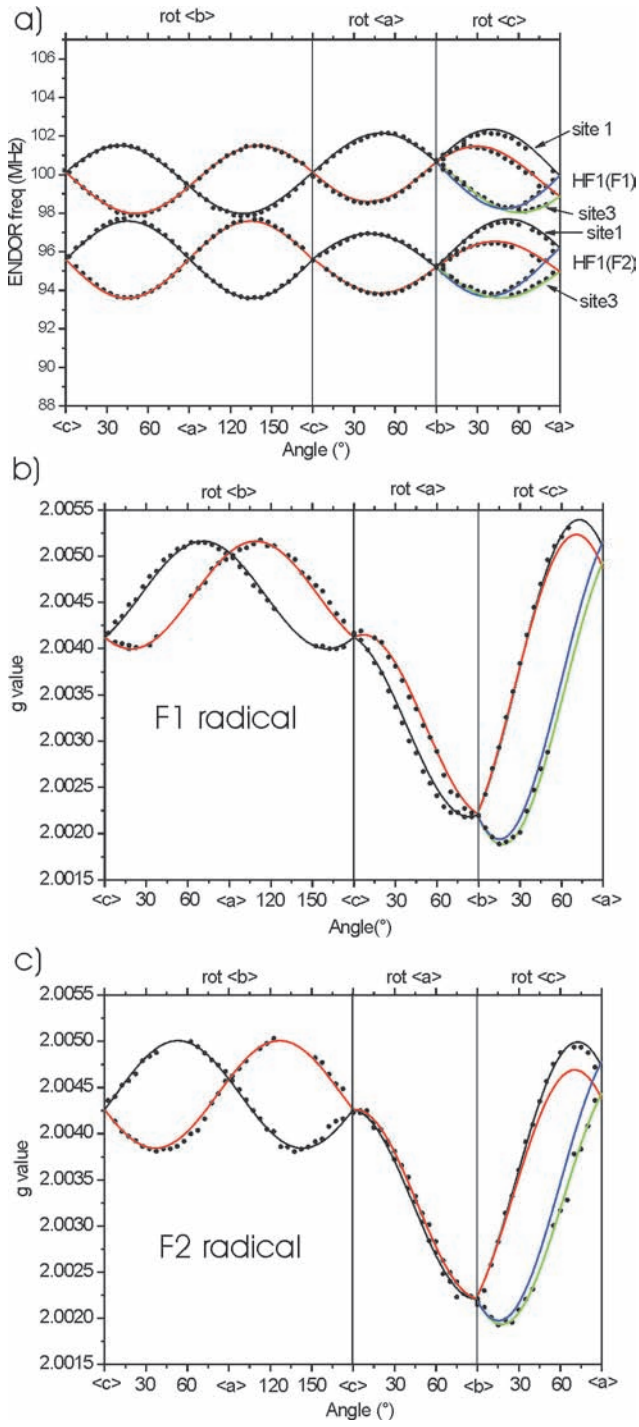

Figure 4. (a) ENDOR line angular variation in the three rotation planes for the HF1(F1) and HF1(F2) hyperfine interactions. The circles represent the experimental points, and the solid lines are the simulations using the data in Table 1. (b, c) Angular dependence of g_{eff}-values for the radicals F1 and F2 calculated from the centers of the EIE spectra. The filled circles represent the experimental points, and the solid lines are the simulations using the **g** tensor data in Table 1.

where θ is the dihedral angle between the $2p_z$ lone-electron orbital (LEO) axis and the $C_\beta-H_\beta$ bond, viewed along the $C_\alpha-C_\beta$ bond, ρ^π is the spin density in the LEO orbital and B_0 and B_2 are empirical constants, for which values of 0 and 126 MHz can be assumed in the present case.[29] A minimum spin density ρ^π of about 0.75 is required to yield the isotropic value of HF1(F1), which is still compatible with the presence of a carbonyl group.

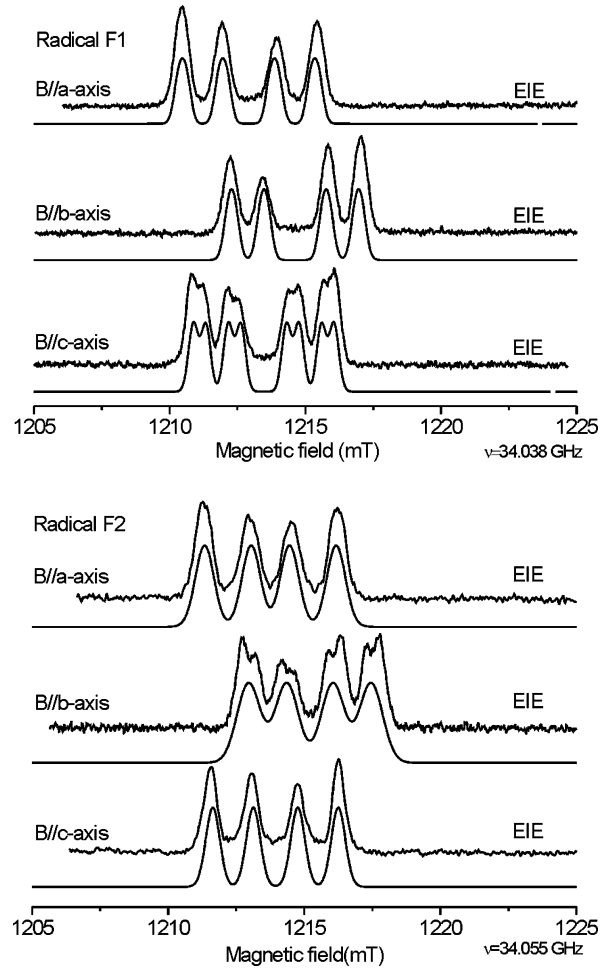

Figure 5. Q-band EIE spectra of RT X-irradiated fructose single crystals for the magnetic field along crystallographic axes. Each experimental spectrum is accompanied by its simulation using the data in Table 1.

The hyperfine coupling of the beta proton in a H−C═O group typically has a small (and sometimes even negative) isotropic component ($a^\beta_{iso} \leq 3G$),[14] which is clearly not the case for HF1 or HF2. The only possibility left then is a fragment of the type

$$R1CH_2-\dot{C}-(C{=}O)-R2 \qquad (I)$$

where the two beta protons are bound to the same carbon atom. Assuming a spin density of 0.8, the McConnell relation (eq 1) yields dihedral angles $\theta_1 = 13°$ for HF1(F1) ($a^\beta_{iso} = 96$ MHz) and $\theta_2 = 52°$ (or $180° - 52° = 128°$) for HF2(F1) ($a^\beta_{iso} = 37$ MHz). Hence the angle between the two C−H bonds is 115°, which is a very plausible value for the case of two beta protons located on the same carbon atom.

Having identified a generic radical fragment that would produce the **g** and proton hyperfine tensors that are experimentally observed, we may now try and fit this in the fructose molecule and crystal structure. To this end, we first analyze the orientations of the proton HF tensors. The eigenvector associated with the largest principal value of a beta or gamma coupling ($b_{+,dip}$) lies approximately along the $C_\alpha\cdots H_\beta$ or $C_\alpha\cdots H_\gamma$ direction. Since F1 and F2 are radicals obtained after RT irradiation, large structural reorientations might be expected, so that the gamma proton coupling is more reliable for comparison with the crystallographic data. The smallest angular

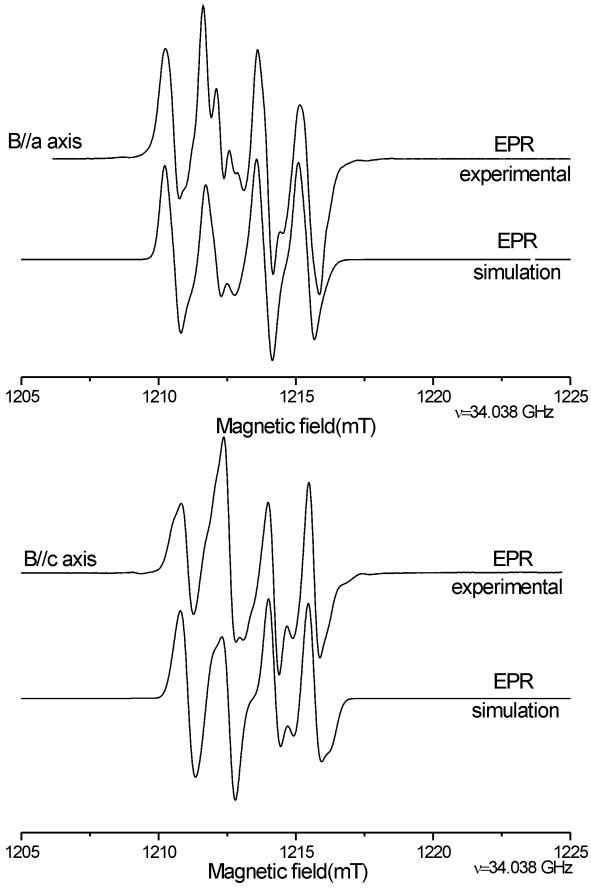

Figure 6. Experimental and simulated (using the data in Table 1) Q-band EPR spectra of RT X-irradiated fructose single crystals for the magnetic field along the *a* and *c* axes.

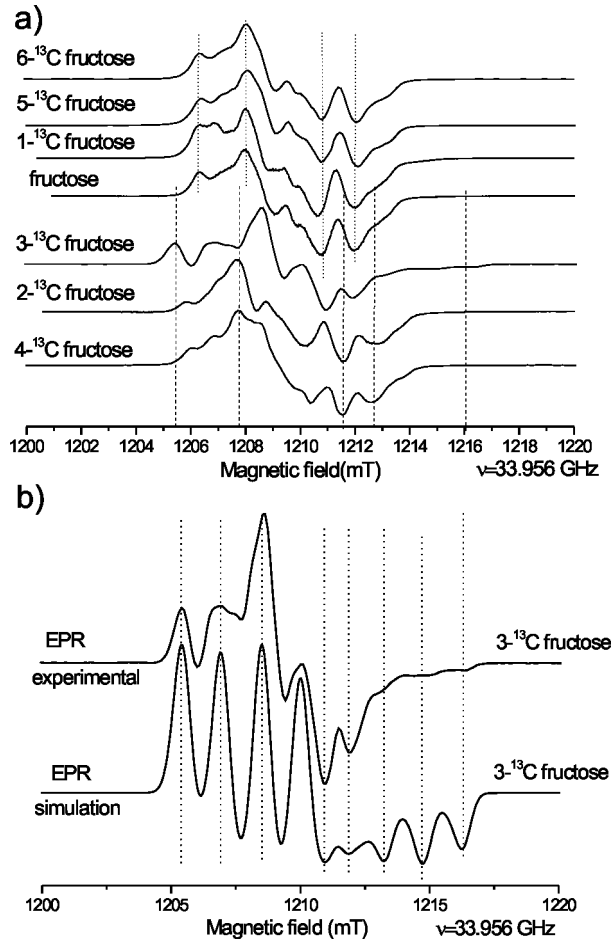

Figure 7. (a) Q-band EPR spectra recorded at 55K of RT X-irradiated β-D-fructose powder with natural abundances of the C isotopes and fructose powder enriched in ^{13}C at different carbon positions. (b) Comparison between the experimental and the simulated spectra for the 3-^{13}C fructose powder.

difference ($\Delta\psi$) between the $b_{+,\mathrm{dip}}$ eigenvector of HF3(F1) and C$\cdots$H$_\gamma$ directions is found for the following cases: C1$\cdots$HC3 ($\Delta\psi = 10°$), C3$\cdots$HC1 ($\Delta\psi = 13°$), C3$\cdots$H′C1 ($\Delta\psi = 16°$) and C2$\cdots$HC4 ($\Delta\psi = 13°$). The most plausible radical centers thus are C1, C2 and C3. A C1 centered radical of type I would demand severe structural alterations. We will therefore only consider C2 and C3 centered radical models here. The carbonyl groups can most easily be formed at C3, C4 and C2 respectively.

The **g** tensor contains important additional information about the radical geometry: the $g_{\min}$ principal direction lies along the LEO axis, which is expected to be roughly perpendicular to the plane formed by the three carbon atoms in fragment I, and the $g_{\max}$ value is approximately parallel to the C═O bond axis, which can be approximated by the external bisector of the angle made by the three carbon atoms in I. The $g_{\min}$ eigenvector makes an angle ($\Delta\psi$) with the vector perpendicular to the C2−C3−C4 plane of 25° for F1 and 32° for F2. For O6−C2−C3, one finds $\Delta\psi = 18°$ for F1 and $\Delta\psi = 30°$ for F2. The $g_{\max}$ eigenvector deviates by 26° from the C2−C3−C4 bisector (in the case of C3═O) and by 34° from the C3−C4−C5 bisector (in the case of C4═O). It was not possible to determine the direction of the C2═O bond, because the formation of the carboxyl group at the C2 position will lead to an open ring structure obtained by the rupture of the C2−O6 bond. All these values are, given the approximations made, acceptable but do not allow discriminating between C2 and C3 as possible radical centers.

The EPR results for the selectively enriched samples at different carbon positions corroborate the reasoning made above: they indicate that the radical center is either C2, C3 or C4 and favor C3 over C2 and C4. All the previous considerations lead us to propose two possible fragments with the general structures $R_1-C4H_2-\dot{C}3R_2-(C2{=}O)-C1HR_3R_4$ and $R_1-(C4{=}O)-\dot{C}3R_2-C2H_2-C1HR_3R_4$. These both are open-ring structures with the two beta protons bound to the same carbon atom, the unpaired electron localized mainly on the C3 atom, and with a plausible candidate for a gamma proton (HC1). The former is perhaps the best candidate since the delocalization onto the carbonyl group at C2 would explain the relatively large principal values of the gamma coupling (HF3(F1)/HF3(F2)). Note that, next to a ring-opening event and the formation of carbonyl group, substitution of one or two hydroxy groups by a hydrogen atom is required. The structural alterations are quite extensive, and no easy formation mechanisms can readily be constructed.

The above reasoning, based on semiempirical relations for interactions in carbohydrate radicals and data of previously identified radicals, do not lead to a positive identification of the structure of F1 and F2. Apparently, more advanced quantum chemical modeling, taking among others also the crystalline environment of the radical adequately into account, will be necessary. The additional experimental parameters determined in this work, the **g** tensors and ^{13}C HF data, put additional constraints on models to be considered. In the mean time, the study of radicals with intermediate stability, obtained by annealing crystals irradiated at lower temperatures (10 K and 77 K) or observed immediately after irradiation at RT, eventually evolving toward the final stable products, may provide informa-

tion on the structure of the latter and on the radiation−chemical pathway toward them.

Conclusions

From the angular dependence of EIE spectra at Q-band, the **g** tensors for the two dominant stable radicals, F1 and F2, in X-irradiated fructose single crystals have been determined. The relatively large *g* anisotropy observed for both radicals might indicate delocalization of the unpaired electron onto a neighboring oxygen atom. Powder EPR measurements on ^{13}C enriched samples suggest that the unpaired electron density is mainly localized at the C3 position. This observation, as well as the relatively large *g* anisotropy, cast doubt on the C2-centered model, obtained by OH abstraction, proposed in a previous study. Taking into account the hyperfine tensors determined previously, the **g** tensors determined in the present study and the measurements on the selectively enriched samples, two new possible radical fragments were proposed.

Acknowledgment. The authors wish to acknowledge the Flemish Research Foundation (FWO) for the financial support.

References and Notes

(1) Madden, K. P.; Bernhard, W. A. *J. Phys. Chem.* **1979**, *83* (20), 2643.

(2) Pauwels, E.; Van Speybroeck, V.; Callens, F.; Waroquier, M. *Int. J. Quantum Chem.* **2004**, *99* (2), 102.

(3) Vanhaelewyn, G. C.A.M.; Lahorte, P. G. A.; De Proft, F.; J, A.; Geerlings, P. F. C.; Mondelaers, W. K. P. G.; Callens, F. J. *Phys. Chem. Chem. Phys.* **2001**, *3* (9), 1729–1735.

(4) Vanhaelewyn, G. C. A. M.; Pauwels, E.; Callens, F. J.; Waroquier, M.; Sagstuen, E.; Matthys, P. *J. Phys. Chem. A* **2006**, *110*, 2147.

(5) Tarpan, M.; Sagstuen, E.; Pauwels, E.; Vrielinck, H.; Waroquier, M.; Callens, F. *J. Phys. Chem. A* **2008**, *112*, 3898.

(6) Vanhaelewyn, G.; Sadlo, J.; Callens, F.; Mondelaers, W.; De Frenne, D.; Matthys, P. *Appl. Radiat. Isot.* **2000**, *52*, 1221.

(7) De Cooman, H.; Pauwels, E.; Vrielinck, H.; Dimitrova, A.; Yordanov, N.; Sagstuen, E.; Waroquier, M.; Callens, F. *Spectrochim. Acta A* **2008**, *69*, 1372.

(8) Box, H. C.; Budzinski, E. E.; Freund, H. G. *J. Chem. Phys.* **1990**, *121*, 262.

(9) Samskog, P. O.; Lund, A.; Nilsson, G.; Symons, M. C. R. *J. Chem. Phys.* **1980**, *73*, 4862.

(10) Samskog, P. O.; Kispert, L. D.; Lund, A. *J. Chem. Phys.* **1983**, *79*, 635.

(11) Samskog, P. O.; Lund, A. *Chem. Phys. Lett.* **1980**, *75*, 525.

(12) Sagstuen, E.; Lindgren, M.; Lund, A. *Radiat. Res.* **1991**, *128*, 235.

(13) Pauwels, E.; Van Speybroeck, V.; Waroquier, M. *J. Phys. Chem. A* **2006**, *110*, 6504.

(14) De Cooman, H.; Pauwels, E.; Vrielinck, H.; Sagstuen, E.; Callens, F.; Waroquier, M. *J. Phys. Chem. B* **2008**, *112*, 7298.

(15) De Cooman, H.; Pauwels, E.; Vrielinck, H.; Sagstuen, E.; Van Doorslaer, S.; Callens, F.; Waroquier, M. *Phys. Chem. Chem. Phys.* **2009**, *11*, 1105.

(16) De Cooman, H.; Vanhaelewyn, G.; Pauwels, E.; Sagstuen, E.; Waroquier, M.; Callens, F. *J. Phys. Chem. B* **2008**, *112*, 15045.

(17) Pauwels, E.; De Cooman, H.; Vanhaelewyn, G.; Sagstuen, E.; Waroquier, M.; Callens, F. *J. Phys. Chem. B* **2008**, *112*, 15054.

(18) Kang, J.; Tokdemir, S.; Shao, J.; Nelson, W. H. *J. Magn. Reson.* **2003**, *165*, 128.

(19) Engalicheff, A.; Kolberg, M.; Barra, A. L.; Anderson, K. K.; Tilquin, B. *Free Radical Res.* **2004**, *38*, 59.

(20) Georgieva, E. R.; Pardi, L.; Jeschke, G.; Gatteschi, D.; Sorace, L.; Yordanov, N. D. *Free Radical Res.* **2006**, *40*, 553.

(21) Kanters, J. A.; Roelofsen, G.; Alblas, B. P.; Meinders, I. *Acta Crystallogr. B* **1977**, *33*, 665.

(22) Takagi, S.; Jeffrey, G. A. *Acta Crystallogr. B* **1997**, *33*, 3510.

(23) Stoll, S.; Schweiger, A. *J. Magn. Reson.* **2006**, *178*, 42.

(24) Schonland, D. S. *Proc. Phys. Soc. London* **1959**, *73*, 788.

(25) Vrielinck, H.; De Cooman, H.; Tarpan, M. A.; Sagstuen, E.; Waroquier, M.; Callens, F. *J. Magn. Reson.* **2008**, *195*, 196.

(26) Sagstuen, E.; Lund, A.; Awadelkarim, O.; Lindgren, M.; Westerling, J. *J. Phys. Chem.* **1986**, *90*, 5584.

(27) McConnell, H. M. *J. Chem. Phys.* **1956**, *24*, 764.

(28) Heller, C.; McConnell, H.M. J. *Chem. Phys.* **1960**, *32*, 1535.

(29) Morton, J. R. *Chem. Rev.* **1964**, *64*, 453.

JP9017019